

# Many-body correlations and Isospin equilibration in multi-fragmentation processes

M.Papa<sup>a)\*</sup> and G.Giuliani<sup>b)</sup>

*a) Istituto Nazionale Fisica Nucleare-Sezione di Catania,*

*V. S.Sofia 64 95123 Catania Italy and*

*b)Dipartimento di Fisica e Astronomia,*

*Università di Catania V. S.Sofia 64 95123 Catania Italy*

## Abstract

Isospin equilibration in multi-fragmentation processes is studied for the system  $^{40}\text{Cl} + ^{28}\text{Si}$  at 40 MeV/nucleon. The investigation is performed through semiclassical microscopic many-body calculations based on the CoMD-II model. The study has been developed to describe isospin equilibration processes involving the gas and liquid "phases" of the total system formed in the collision processes. The investigation of the behavior of this observable in terms of the repulsive/attractive action of the symmetry term, highlights many-body correlations which are absent in semiclassical mean-field approaches.

PACS numbers: 25.70.Pq, 02.70.Ns, 21.30.Fe, 24.10.Cn

---

\* e-mail: papa@ct.infn.it

An interesting subject related to the Heavy Ions Isospin physics [1] is the process leading to the equilibration of the charge/mass ratio between the main partners of the reaction. The so called "isospin diffusion" phenomenon has been indicated as the associated mechanism acting between the reaction partners [2, 3, 4, 5]. In particular, in basically binary processes occurring after the collision of  $Sn$  124 and 112 isotopes [3], evidence of partial equilibrium in the charge/mass ratios of the quasi-projectile (QP) and quasi-target (QT) has been deduced through the study of the iso-scaling parameters related to the isotopic distributions. In this case dynamical calculations based on the BUU model [6] show that the degree of equilibration depends on the behavior of the symmetry potential  $U^\tau$  as a function of the density. The analysis in this kind of studies, however, is based on the linear relation between the iso-scaling parameter and the relative neutron excess  $Y$  of the emitting sources (an assumption typical of several statistical models), moreover, it is also assumed that both quantities weakly depend on the secondary statistical decay processes. However, in general, this last condition depends on the fragment excitation energies, or temperatures, and on the distinctive features of the models used to simulate the second stage decay [7]. In this work we want to describe the isospin equilibration process, looking at the whole system, by using the dynamical variable  $\vec{V}(t) = \sum_{i=1}^{Z_{tot}} \vec{v}_i$ . The sum on the index  $i$  is performed on all the  $Z_{tot}$  protons of the system.  $\vec{V}(t)$  corresponds to the time derivative of the total dipole of the system. The velocities  $\vec{v}_i$  are computed in the center of mass (c.m.) reference system. Several studies were based on this dynamical variable to describe pre-equilibrium  $\gamma$ -ray emission (see Refs.[8, 9, 10, 11] and references therein ). Various reasons dictate this choice to describe also isospin equilibration processes.

- i) After the pre-equilibrium stage at the time  $t_{pre}$ , when a second stage characterized by an average isotropic emission of the secondary sources (statistical equilibrium) takes place, the ensemble average satisfies the following relation:  $\overline{\vec{V}}(t_{pre}) = \overline{\vec{V}}(t > t_{pre}) \equiv \overline{\vec{V}}$  [9]. The average value of the dynamical variable at  $t_{pre}$  is in fact invariant with respect to statistical processes and therefore  $\overline{\vec{V}}$  is an interesting observable to be investigated. In particular,  $\overline{\vec{V}}$  can be expressed as function of the charge  $Z$ , mass  $A$ , average multiplicity  $\overline{m}_{Z,A}$  and the mean momentum  $\langle \vec{P} \rangle_{Z,A}$  of the detected particles having charge  $Z$  and mass  $A$  in the generic event:

$$\overline{\vec{V}} = \sum_{Z,A} \frac{Z}{A} \overline{m}_{Z,A} \langle \vec{P} \rangle_{Z,A} C_{\langle \vec{P} \rangle}^{Z,A} \quad (1)$$

$$C_{\langle \vec{P} \rangle}^{Z,A} = \frac{\overline{m_{Z,A} \langle \vec{P} \rangle_{Z,A}}}{\langle \vec{P} \rangle_{Z,A} \overline{m_{Z,A}}} \quad (2)$$

$C_{\langle \vec{P} \rangle}^{Z,A}$  is the correlation function between the multiplicity and the mean momentum. This correlation function plays a determinant role for the invariance property and therefore asks for an analysis event by event in which many-body correlations can not be neglected.

$\overline{\vec{V}}$ , for symmetry reasons, lie on the reaction plane. As suggested from Eq.(1), it is directly linked with a weighted mean of the charge/mass ratio. It takes into account also the average isospin flow direction through the momenta  $\langle \vec{P} \rangle_{Z,A}$ .

-ii) In the general case, we find attractive the following decomposition:  $\overline{\vec{V}} = \overline{\vec{V}}_G + \overline{\vec{V}}_L + \overline{\vec{V}}_{GL}$  where with  $\overline{\vec{V}}_G$  and  $\overline{\vec{V}}_L$  we indicate the dipolar signals associated to the gas "phase" (light charged particles) and to the "liquid" part, corresponding to the motion of the ensemble of the produced fragments (QP,QT, if any, and intermediate mass fragments). The signal  $\overline{\vec{V}}_{GL}$  is instead associated to the relative motion of the two "phases". By supposing, for simplicity, that the gas "phase" is formed by neutrons and protons,  $\overline{\vec{V}}$  can be further decomposed as:

$$\overline{\vec{V}} = \frac{A_G(1 - Y_G^2)}{4} \overline{\vec{v}}_r^{NP} + \frac{\mu_{G,L}(Y_L - Y_G)}{2} \overline{\vec{v}}_{cm,LG} + \overline{\vec{V}}_{r,L} \quad (3)$$

In the above expression the first term represents the contribution related to the neutron-proton relative motion of the gas "phase" expressed through the relative velocity  $\overline{\vec{v}}_r^{NP}$ , the second term is related to the relative motion  $\overline{\vec{v}}_{cm,LG}$  between the centers of mass of the "liquid" complex and the "gas"; the last term represents the contribution produced by the relative motion of the fragments. A similar expression can be obtained including in the gas "phase" other light particles. From this decomposition we can see how the isospin equilibration condition ( $\overline{\vec{V}} = 0$ ), for the total system, requires a very delicate balance which depends on the average neutron excess of the produced "liquid drops"  $\overline{Y}_L$ , on the one associated to the gas "phase"  $\overline{Y}_G$  and on the relative velocities between the different parts. To enlighten the role played by some of the terms reported in Eq.(3), we can discuss the idealized decay of a charge/mass asymmetric source through neutrons and protons emission (or the case in which the liquid drops are produced through a statistical mechanism  $\overline{\vec{V}}_{r,L} = 0$ ). Moreover, for simplicity, we can consider uncorrelated fluctuations between the velocities and neutron excesses. In absence of pre-equilibrium emission or for identical colliding nuclei ( $\overline{\vec{v}}_{cm,LG} = 0$ ) the second term of Eq.(3) is zero, and the isospin equilibration will require a

proton-neutron symmetric gas "phase" and/or absence of relative neutron-proton motion. For non identical colliding nuclei, if pre-equilibrium emission is present, then  $\overrightarrow{v}_{cm,LG} \neq 0$ . In this case, if  $\overline{Y}_G \neq \overline{Y}_L$ , as due to the isospin "distillation" phenomenon, the first term has to be necessarily different from zero and it will contribute to the neutron-proton differential flow  $F_{np}$  (see the following). Therefore, for the whole system, the isospin equilibration process can not be explained only in terms of isospin diffusion and drift between the main partners of the reaction. It is in fact necessary to take into account the gas "phase" contribution which we can regard as a kind of "dissipation" with respect to the system formed by the liquid part. In particular in this work, as an example, we will discuss the results obtained through the Constrained Molecular Dynamics-II approach (CoMD-II) [12, 13] applied to the charge/mass asymmetric system  $^{40}\text{Cl} + ^{28}\text{Si}$  at 40 MeV/nucleon. The study is performed by using different options for the symmetry potential term  $U^\tau$ . Nevertheless, to clearly understand the dynamics of the investigated system, it is necessary to dedicate the following part to a discussion of this term. In particular, we will illustrate that the existence of many-body correlations, as produced in our approach, strongly affects this part of the interaction.

In the framework of the present version of the CoMD-II model the isospin momentum dependent part of the total energy is included through the Pauli principle constraint and the potential symmetry term has been implemented as follows [8, 13]:

$$U^\tau = \frac{a_{sym}}{2s_{g.s.}} F'(s) \beta_M \quad (4)$$

$$\beta_M = \rho^{NN} + \rho^{PP} - \rho^{NP} - \rho^{PN} \quad (5)$$

$$\rho^{KK'} = \sum_{\substack{i \subseteq K, j \subseteq K \\ i \neq j}} \rho_{i,j} \quad K, K' = N \text{ or } P \quad (6)$$

$$F'(s) = \frac{2s}{s_{g.s.} + s} \quad \text{Stiff1} \quad (7)$$

$$F'(s) = 1 \quad \text{Stiff2} \quad (8)$$

$$F'(s) = \left(\frac{s}{s_{g.s.}}\right)^{-\frac{1}{2}} \quad \text{Soft} \quad (9)$$

$$s = \frac{4}{3A} \sum_{\substack{i, j \subseteq K \cup K' \\ i \neq j}} \rho_{i,j} \quad (10)$$

With the superscript N and P we indicate the neutron and the proton ensemble of nucleons respectively and A is the total mass of the system.  $\rho_{i,j}$  represents the normalized Gaussian overlap matrix elements [12] typical of the quantum molecular dynamics approach [14]. The label  $g.s.$  indicates the ground state configuration. The positive form factors  $F'(s)$  are

such that  $F'(s)\frac{s}{s_{g.s.}}$  has the same functional form like  $F(u)$  proposed in [15] (see Eq.(3) in Ref.[15]). They have been used extensively in mean-field (M.F.) approaches. Apart from a normalization factor, equal to  $\frac{4}{3}$ ,  $s$  is related to the average (with respect to the number of two-body interactions) overlap integral. For the system under study and for compact configurations  $s$  is well approximated by the average one-body density  $\rho$ . The factor  $\beta_M$  instead arises naturally from the many-body approach. It takes into account explicitly, through the last two negative terms in Eq.(5), that the microscopic two-body nucleon-nucleon interaction in the isospin singlet states is more attractive than the one related to triplet states [8] ( $a_{sym} = 72MeV$ ). For the moderately asymmetric system, here investigated, self-consistent calculations, including the ones for the searching of the g.s. properties, produce a negative value of  $\beta_M$ . This result is due to the combined actions of the more attractive force, for the isospin singlet states, and the repulsive action of the Coulomb interaction for proton-proton couples. We have verified also that the Pauli principle plays a role even if with a smaller extent. These correlations, in fact, tend to increase the average (with respect the number of two-body interactions) neutron-proton overlap integral  $\tilde{\rho}^{NP}$  and to decrease the overlap  $\tilde{\rho}^{PP}$  and  $\tilde{\rho}^{NN}$  related to the neutron-neutron and proton-proton couples. These average overlap integrals are defined as:  $\tilde{\rho}^{II'} = \rho^{II'}/II'$  with  $I$  and  $I'$  equal to  $N$  and/or  $P$ . In our calculations we have verified that  $\tilde{\rho}^{NP} = \tilde{\rho}^{PN} \equiv \alpha \frac{(\tilde{\rho}^{PP} + \tilde{\rho}^{NN})}{2}$  with  $\alpha \simeq 1.1 - 1.2$ . Therefore, at low asymmetry, it is enough a small correlation effect to produce a negative value of  $\beta_M$ , as due to the structure of Eq.(5). However, it results that  $\beta_M$  decreases by increasing the symmetry of the system (the number of singlet states increases) and, on the contrary, it increases by decreasing the symmetry of the system. These changes follow a parabolic dependence with respect the  $\chi = N - Z$  variable. This means that  $\beta_M$  contains, independently from the sign, the right behavior necessary to explain the differences in the binding energies of isobars nuclei and it is able to generate the so called "isospin distillation" phenomenon [5] in the dynamics of hot sources. However, the negative sign of  $\beta_M$  has relevant consequences in to determine the effects of the different options for  $U^\tau$  on the dynamics of the investigated processes. For example, contrary to the semi-classical M.F. description, the so called Stiff cases (in spite of this change of sign, we retain the same nomenclature to indicate the different options) show a decreasing behavior with the density. The Soft case, here investigated, even if negative, maintains the increasing pattern typical of a M.F. approach (see Fig.5(c)). We conclude this part by briefly describing how in

M.F. and/or in Liquid Drop Model these correlations are washed out. For this purpose we assume, for simplicity,  $A, N, Z \gg 1$ , and we rewrite  $\beta_M$  as:  $\beta_M = N^2 \tilde{\rho}^{NN} + Z^2 \tilde{\rho}^{PP} - 2NZ \tilde{\rho}^{NP}$ . *M.F. approximation is now easily obtained by supposing  $\tilde{\rho}^{II'} = \frac{\sum_{i \neq j=1}^A \rho_{i,j}}{A^2} \equiv \tilde{\rho} = \frac{3}{4A} \rho$  to be independent on  $I$  and  $I'$ .* This means that the correlation producing the aforementioned differences in the matrix elements  $\tilde{\rho}^{II'}$  are averaged through the overlap integral  $\tilde{\rho}$ , so that:  $\beta_M \rightarrow \frac{3}{4} \frac{\rho}{A} (N - Z)^2 = \frac{3}{4} \rho^2 V \frac{(\rho_n - \rho_p)^2}{\rho^2}$ , where  $\rho_n$ ,  $\rho_p$  and  $\rho$  represent the neutron, proton and total densities respectively.  $V$  is the volume. In this case, therefore, we obtain that the interaction depends locally only through one-body densities and it is positive defined. Taking into account that for the present system, in compact configurations,  $s \cong \rho$ , by substituting the right end of the above relation in Eq.(4) and dividing by the volume  $V$ , we get a precise correspondence with the symmetry energy density used in Ref.[15] if  $e_0 = 27 \text{ MeV}$ . This value includes the reduction of the Fermi motion as due to finite size effects and corresponds to an  $S_0$  value (see Eq.(4) of Ref.[15]) of about 36 MeV. Finally we note that these correlations not only change the sign of the symmetry energy, but they heavily affect also the strength. In particular, according to Eqs.(4-10) and to the definition of  $\beta_M$  in terms of the average overlap integral  $\tilde{\rho}^{II'}$  it is straightforward to evaluate the contribution of  $\beta_M$  by assuming 10% of correlation, i.e.  $\alpha = 1.1$ . By considering a total system like the one investigated in the present work ( $A=68$   $Y=0.088$ ) at normal density we obtain  $\beta_M \simeq -0.43 \text{ fm}^{-3}$  in the correlated case and  $\beta_M = 0.065 \text{ fm}^{-3}$  in the M.F case. According to this evaluation we observe that also with a correlation value of the order of 1% the induced effect on the symmetry term is not negligible. This strongly suggests that the qualitative effects discussed in the present work can be still present by using other kinds of effective interactions. We have to note also that, according to the increasing behavior of the symmetry energy with the charge/mass asymmetry, for systems with mass around 64 units, the  $\beta_M$  factor becomes positive for relevant asymmetry  $|Y_c| > 0.25$  restoring the repulsive behavior of the asy-stiff cases here investigated.

Now we can discuss the results concerning the isospin equilibration process for the system  $^{40}\text{Cl} + ^{28}\text{Si}$  at 40 MeV/nucleon. For the system under study, in Fig. 1(a) and Fig. 1(b) we show the average total dipolar signals as evaluated through CoMD-II calculations along the  $\hat{z}$  beam direction  $\overline{V}^z$  and along the impact parameter direction  $\hat{x}$ ,  $\overline{V}^x$ , respectively. The reference frame is the c.m. one. The impact parameter  $b$  is equal to 4 fm.

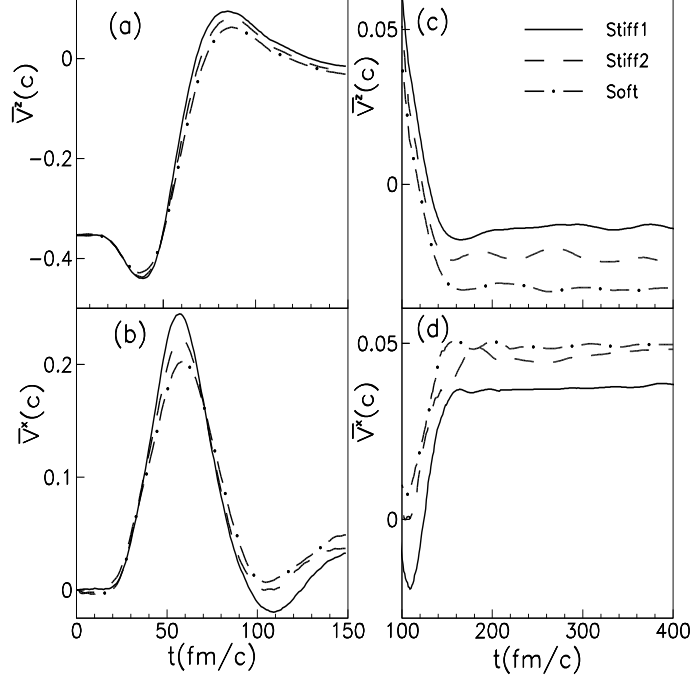


FIG. 1: Average dipolar signals along the  $\hat{z}$  and  $\hat{x}$  directions are plotted as a function of time in the intervals 0-150 fm/c (panels (a) and (b)) and 100-400 fm/c. The three kinds of lines refer to the different options (see eqs.(7-8)) describing the symmetry potential.

In these figures the average dipolar signals are shown for the first 150 fm/c. Different lines refer to different symmetry potentials. The isospin independent compressibility is equal to 220 MeV according to Ref. [12]. In the first 150 fm/c we can see that in all the cases wide oscillations are present. They are responsible for the pre-equilibrium  $\gamma$ -rays emission [8, 9]. The damped oscillations tend to smaller and constant values (within the uncertainty of the statistics of the ensemble average procedure) as can be seen in Fig. 1(c) and Fig. 1(d) in which the dynamical evolution is followed from 100 fm/c up to 400 fm/c. The time interval in which the stationary behavior is reached corresponds to the average time for the formation of the main fragments. In Fig. 2(a), for the different symmetry potentials, we plot the charge  $Z$  distributions. The Stiff1 and Stiff2 options clearly show a multi-fragmentation pattern, while for the Soft case the behavior is closer to an exponential trend making reliable a "vaporization" scenario.

We now briefly comment the results already shown in Figs. 1(c) and 1(d). We can see that the asymptotic values sensitively depend on the options used for the symmetry term. For example, concerning the dipolar signal along the  $\hat{z}$  direction, the difference between the

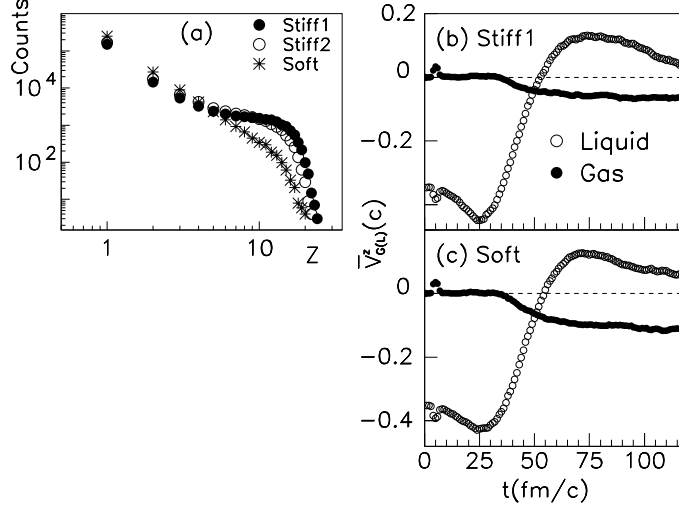


FIG. 2: In the panel (a) we show the charge  $Z$  distributions of the reaction products for the different options describing the symmetry potential (see eqs.(7-8)). In panels (b) and (c), for the Stiff1 and Soft cases, the  $\hat{z}$  components of the dipolar signals are shown for the liquid and gas "phases".

Stiff1 and the Soft cases is about 85% while between the Stiff1 and the Stiff2 options is about 53%. The changes of the dipolar signals along the  $\hat{x}$  direction are smaller of the order of 10-30%. To understand the role of the "gas" particles, in Fig. 2(b) and in Fig. 2(c) we show with open circles and with closed circles the values of dipolar signal along the  $\hat{z}$  direction,  $\bar{V}_G^z$  (gas "phase") as a function of time and  $\bar{V}_L^z$  (liquid "phase"), for the Stiff1 and Soft parameterizations respectively. We can see that the contributions related to the "gas" are negative (light particles coming essentially from the target). They are quite effective in to reduce the absolute value of the total dipolar signals driving the total system through the isospin equilibration. It is also possible to see that  $\bar{V}_G^z$  shows a larger absolute value for the Soft case with respect the Stiff1 option. This is due to the more repulsive effect obtained in the Soft case with respect to the other ones. In Fig. 3(a) we show, as a function of time, the average overlap integral  $s$  for the three cases.

In Fig. 3(b) and Fig. 3(c) we show the corresponding total average potential  $\bar{U}^{tot}$  and the symmetry one  $\bar{U}^r$ . From Fig. 3(a) we can see that the maximum value of  $s$ ,  $s_{max}$ , is reached in about 30 fm/c. The Soft case shows the lower  $s_{max}$  value, the Stiff1 the higher one (about 1.25 times the  $s_{g.s.}$  value). Accordingly,  $\bar{U}^{tot}$  displays the less attractive behavior for the Soft case (see Fig. 3(b)). The reasons of these differences can be understood by looking



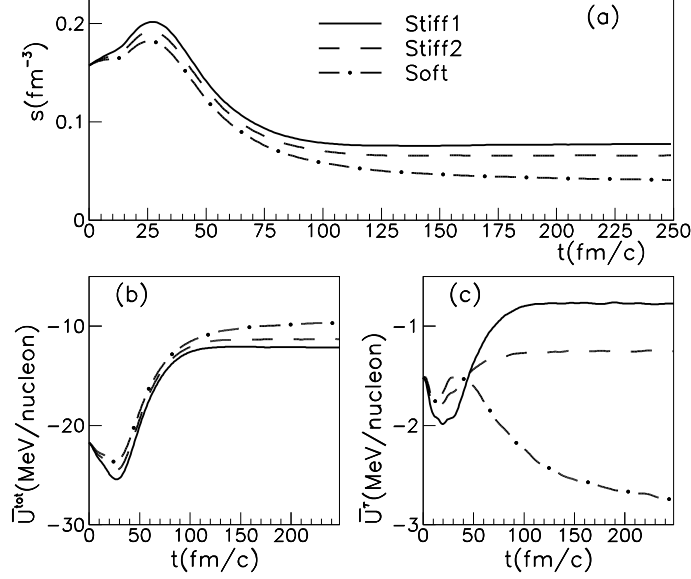


FIG. 3: (a) average overlap integral  $s$ , (b) average total potential, (c) average symmetry potential are shown as a function of time for the different options describing the symmetry potential (see eqs.(7-8)).

at Fig. 3(c).  $\bar{U}^{\tau}$  shows, in fact, a clear repulsive behavior as a function of the density for the Soft case while the Stiff1 case gives rise to an attractive effect. At later times, when the density is decreasing and the fragment formation process takes place for  $s < s_{g.s.}$ , the behavior of  $\bar{U}^{\tau}$  in the different cases is reversed. The Stiff2 case shows always an attractive behavior with intermediate values concerning the strength. The differences observed around 30 fm/c play a crucial role in to determine the later evolution of the system [16]. This can be understood by looking at the figures 2(a) and 2(b). In these figures it is in fact clearly visible that the dipolar signals associated to the gas "phase" start to develop just at 30 fm/c. The less attractive behavior  $\bar{U}^{\text{tot}}$  for the Soft case determines a lower collision rate and a higher multiplicity of light particles. For example, the total number of neutrons and protons emitted at 160 fm/c is, on average, about 15 for the Soft case and 11 for the Stiff1 one. The gas "phase" is more rich in neutron for the Soft case ( $Y_G \cong 0.23$ ) with respect to the Stiff1 option ( $Y_G \cong 0.18$ ). These values are rather large as compared with the neutron excess fraction of the total system and with the one related to the biggest fragment. This clearly indicates the occurrence of the so called "isospin distillation". As above mentioned the dipolar signals associated to the relative neutron-proton motion for the gas "phase" can affect the neutron-proton differential flow  $F_{np}$  [17]. As an example in Fig. 4(a) for the Soft

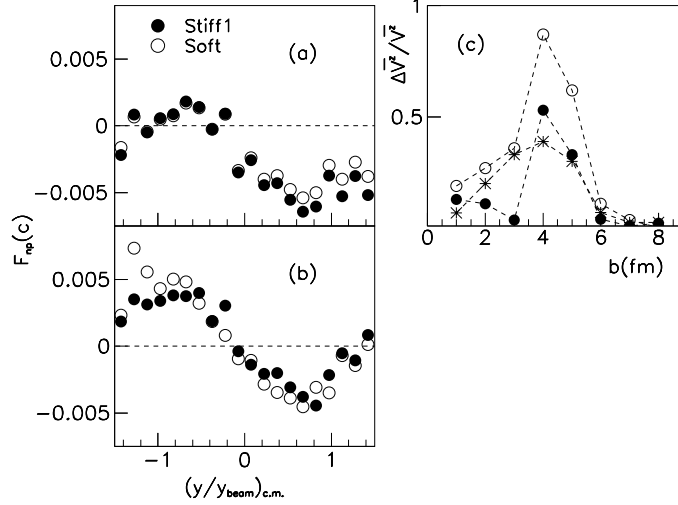


FIG. 4: (a) Differential neutron-proton flow  $F_{np}$  as a function of  $(\frac{y}{y_{beam}})_{c.m.}$  (see text). (b) The same quantity is plotted after the corrections given by the relative neutron-proton motion related to the gas "phase". (c) For different symmetry potentials we show the relative changes  $\frac{\Delta \bar{V}^z}{\bar{V}^z}$  of the average total dipolar signal along the  $\hat{z}$  component as a function of the impact parameter.

and Stiff1 cases we show the neutron-proton differential flow as a function of the particles rapidity  $y$  normalized to the projectile one  $y_{beam}$ .

The rapidity values are evaluated in the c.m. reference system. In Fig. 4(b), we show the same quantities corrected for the average free neutron-proton relative motion. We can see that the differences are considerable and, in this case, they are due essentially to the  $\hat{x}$  component of the relative motion. We conclude this study by showing in Fig. 4(c), for the different symmetry terms, the relative changes  $\frac{\Delta \bar{V}^z}{\bar{V}^z}$  of the average total dipolar signals along the  $\hat{z}$  component as function of the impact parameter. It is clearly visible the higher sensitivity obtained for the impact parameter range  $b \cong 3.5 - 5.5$  fm. CoMD-II calculations show that, for more central collisions, even if the relative changes in the overlap integrals are slightly more pronounced, the increasing of the collision rate produces a more damped mechanism with respect to the dipolar degree of freedom. This determines a smaller sensitivity to the change of the symmetry energy. On the contrary, for more peripheral reactions, the dipolar signal shows a smaller damping and a related smaller degree of equilibration. In this case, however, the changes in the relative overlap integral  $s$  are smaller so that the associated changes in  $\bar{U}^r$  are less pronounced. These suppression mechanisms and the related existence of an optimal range of impact parameters for an enhanced visibility of the isospin

effects seem to us quite general, and clearly depending also on the way in which the collision term is treated [13].

In summary, in this work the isospin equilibration process for the asymmetric charge/mass system  $^{40}\text{Cl} + ^{28}\text{Si}$  at 40 MeV/nucleon has been investigated by studying the ensemble average of the time derivative of the total dipole  $\overline{\overline{V}}$  as evaluated through CoMD-II calculations. Some general properties of this quantity have been discussed. In particular, it allows to give a consistent definition of isospin equilibration also in complex reactions evolving through multi-fragmentation processes. CoMD-II calculations show that the asymptotic values of  $\overline{\overline{V}}$  for these processes are quite sensitive to different symmetry potential options; moreover, for this system, the dipolar contribution associated to the pre-equilibrium charged particles emission is relevant in to determine the value of  $\overline{\overline{V}}$ . Detailed CoMD-II calculations also enlighten fundamental differences in the behavior of the symmetry potential with respect to a description based on a M.F. approach. The negative sign of the leading  $\beta_M$  factor in the symmetry potential represents a typical example in which the ensemble average, performed on many realizations of a semiclassical many-body dynamics approach, gives arise to deep differences with respect to the average behavior evaluated with a M.F. approach. These deviations are due to the highly correlated neutron-proton motion generated by the symmetry term and they are clearly beyond the one-body description. Moreover, the calculations presented in the present work suggest the existence of relevant critical charge/mass asymmetries starting from which the symmetry potential changes sign producing a transition from a density attractive to a density repulsive behavior for the asy-stiff cases. We conclude by observing that this subject needs further detailed studies in the next future together with a specific investigation about the effects of these correlations on the behavior of others isospin-dependent observables.

- 
- [1] W.U.Schröder and J.Töke, in *Nonequilibrium Physics at Short Times*, edited by K.Morawetz, Springer-Verlag, Berlin, Heidelberg, New York, 2004, p.417.
  - [2] L. Shi and P.Danielewicz, Phys. Rev. C. **68** 064604 (2003).
  - [3] Betty Tsang and Lijun Shi, Nucl. Phys. **A738** (2004).
  - [4] Andrew W.Steiner and Bao-An Li, Phys. Rev. C. **72** 041601(R) (2005).

- [5] V.Baran, M.Colonna, M.Di Toro, M.Zielinska-Pfabé and H.H.Wolter, Phys. Rev. C. **72** 064620 (2005).
- [6] G.Bertsh and S.Das Gupta, Phys.Rep. **160**, 189 (1988).
- [7] M.B.Tsang *et al*, Eur. Phys. J. **A30**, 129-139 (2006).
- [8] G.Giuliani and M.Papa, Phys. Rev. C **73**, 031601(R) (2006).
- [9] M.Papa *et al*, Phys. Rev. C **72**, 064608 (2005).
- [10] M.Papa et al, Phys.Rev. **C68** 034606 (2003).
- [11] F.Amorini et al, Phys.Rev. **C69** 014608 (2004).
- [12] M.Papa, T.Maruyama and A.Bonasera, Phys. Rev. C **64**, 024612 (2001) and reference therein.
- [13] M.Papa, G.Giuliani and A.Bonasera, J Comput. Phys.**208**, 403 (2005).
- [14] J.Aichelin, Phys. Rep. **202**, 233 (1991).
- [15] Bao-An Li, C.M.Ko and Zhongzhou Ren, Phys. Rev. Lett **78**, 1644 (1997) and reference therein.
- [16] P.Danielewicz, R.Lacey and W.C.Lynch, *Science***298**, 1592 (2002).
- [17] M.Di.Toro, S.J.Yennello and B.-A. Li, Eur. Phys. J. **A30**, 153-163 (2006).